New Edge-Enhanced Error Diffusion Algorithm Based on the Error Sum Criterion

Jae Ho Kim* Tae Il Chung† Hyung Soon Kim* Kyung Sik Son*
Pusan National University Image and Communication Laboratory
San 30, Jangjeon, Kumjung Pusan, Korea 609-735

Yoon Soo Kim Samsung Electronics Company, Ltd.
Visual Communications Laboratory, Suwon P.O. Box 150
Suwon, Korea 440-600

Abstract

A new edge-enhanced error diffusion algorithm, based on Eschbach's algorithm, is proposed. Thick-edged artifacts as well as small edge-enhancement effects for the bright or dark pixel values are observed in the previous algorithm. By analyzing the phenomena, a new improved algorithm is proposed by using the diffused error sum and input pixel value. An input pixel is classified into a normal- or edge-region pixel based on the error sum criterion. A new error calculation is then employed for the edge-region pixel, while conventionel error calculation is used for the normal-region pixel. The proposed method requires only a few additional calculations and provides edge-enhanced binary output images. The edges are influenced less by the brightness offset, and thick-edged artifacts are reduced.

1 Introduction

The development of digital halftoning technology[1–10] allowed for better printed images with only black and white information. This technology has a wide range of application areas such as in facsimile machines, digital copiers, and color printers. Related research has recently increased[3–10] because it is a key technology for low-cost color facsimile machines, color copiers, and digital copiers.

One of the most outstanding halftoning methods is the error diffusion (EDF) technique.[1] In this method, the binarization error for an input pixel is distributed to generate output images. It is excellent for reproducing gray-scale images and has good edge characteristics.[1,3] The error-diffused binarization shows better image quality for the human viewer than the fixed dither method, but it requires more calculations. With the recent advances in processor design technology, the EDF technique becomes a good, realizable solution.[11]

One must consider that the scanner unit has low-pass filtering. This filtering is represented by the modulation transfer function (MTF). In the MTF, the current leakage of a CCD sensor cell into the adjacent cells is considered as well as other optically related blurring effects.[11] In some scanner units, high-pass filtering is used to restore the original images. However, the computational overhead for making the high-pass filtered image is large and the required memory size is also significant. The restoration procedure for binarization can be combined with the EDF process to achieve cost-effective implementation.

Among the several attempts at edge-enhanced binarization, Eschbach's edge enhancing method given in Ref. 4 is one of the most useful from the implementation point of view. It uses only one pixel input value and two line error values. Eschbach generously used input brightness dependent thresholds for developing edge-enhanced binarization.[4] The error calculation scheme is the same as that of the conventional EDF process. It is excellent because only a slight change in the ordinary EDF structure is necessary and only a small amount of additional calculation is needed.

After reviewing Eschbach's edge-enhancing method, it was found that the edge-enhancement effect is related not only to the brightness difference of the adjacent pixels but also to the input pixel brightness itself. This is because the EDF effect of data outside of the dynamic range has not been considered. The thick-edged artifacts became visible as the edge-enhanced factor increased. Without solving these problems, the edge-enhanced EDF is hard to apply to mixed input images, including text and photos. Characters in a magazine sometimes have colored backgrounds that induce offset brightness, which is one of the document styles that needs to be processed.

In Sec. 2, the EDF algorithm and Eschbach's edge-enhanced EDF are briefly explained. In Sec. 3, the problem and the reasons for the problem in Eschbach's method are discussed. In Sec. 4, the relationship between the diffused error sum and input pixel brightness is analyzed. The *reference error sum* E_r^* and the *error sum displacement threshold* W_t, for the input pixel brightness are defined. By using this information, each pixel is classified as a normal- or edge-region pixel. For the edge-region pixels, a new error calculation is used in the proposed algorithm. The analysis of the edge-enhance-

ment characteristics and the corresponding results for the real images are discussed in Sec. 5. In the proposed method, unusual white or black thick-edged artifacts are reduced although the edge-enhancing factor is increased. The effect no longer depends on the brightness offset of the input image.

2 Error Diffusion and Eschbach's Edge-Enhanced EDF Algorithm

In the EDF algorithm, the error created as a result of the pixel binarization is distributed with a certain ratio called an *error filter*. The distributed error to adjacent pixels is summed with the current pixel brightness for determining the output value. In the conventional EDF algorithm,[1] the modified input pixel brightness $I_c(x,y)$ is calculated from the input $I(x,y)$ and the error of adjacent pixels $E(\bullet,\bullet)$. It is expressed as follows:

$$I_c(x,y) = I(x,y) + \frac{\sum_{i,j} \alpha_{i,j} E(x - i\Delta x, y - j\Delta y)}{\sum_{i,j} \alpha_{i,j}}, \quad (1)$$

where x, y, Δx, and Δy are the horizontal axis, the vertical axis of the image, x directional pixel size, and y directional pixel resolution, respectively. The set of coefficients $\alpha_{i,j}$ is called an error filter, suggested by Floyd,[1] and is expressed as:

$$\mathbf{A} = \begin{bmatrix} — & * & \alpha_{1,0} \\ \alpha_{-1,1} & \alpha_{0,1} & \alpha_{1,1} \end{bmatrix} = \begin{bmatrix} — & * & 7 \\ 3 & 5 & 1 \end{bmatrix}. \quad (2)$$

For this error filter, many variations have been suggested for improving image quality. In this paper, the error filter defined in Eq. (2) is utilized because it is widely used and simple to implement.

The modified input pixel brightness is $I_c(x,y)$. The resulting binary output $O_b(x,y)$ and the error $E(x,y)$ are expressed by the following Eqs. (3) and (4), respectively:

$$O_b(x,y) = \Theta\big[I_c(x,y) - T_0\big] = \begin{cases} 255(\text{white}) & I_c > T_0 \\ 0(\text{black}) & I_c \leq T_0 \end{cases}, \quad (3)$$

$$E(x,y) = I_c(x,y) - O_b(x,y), \quad (4)$$

where $\Theta[\bullet]$ and T_0 are the binarization function and a threshold for the binarization, respectively. The center value of the white (255) and the black (0) is used for the threshold in the ordinary EDF. Although one changes the threshold, the statistical behavior of the resulting binary output is not influenced in the EDF algorithm. This improves the image quality by periodically modulating the real threshold.[12] Eschbach has implemented an edge-enhanced EDF using a threshold that depends on the input-pixel brightness.[4]

A new input-dependent threshold is defined as

$$T(I) = T_0 - (K - 1) * I(x,y), \quad (5)$$

instead of the fixed T_0 of Eq. (3). Note that K in Eq. (5) determines the degree of the edge enhancement and is called an *edge-enhancing factor*. Eschbach's edge-enhanced EDF is expressed in Eq. (6). The output value of Eschbach's EDF is determined by

$$O_b(x,y) = \Theta\big[I_c(x,y) - T(I)\big] = \begin{cases} 255(\text{white}) & I_c > T(I) \\ 0(\text{black}) & I_c \leq T(I) \end{cases}. \quad (6)$$

In this case, the error calculation is performed by Eq. (4), which is the same as the conventional EDF. If the edge-enhancing factor is 1, Eschbach's EDF is the same as the ordinary EDF. As K increases, the edges of the image become more visible. The structure change of this algorithm compared to the ordinary EDF is small and only a few additional calculations are required.

3 Problems with Edge Enhancement in Eschbach's Algorithm

Several experiments using various images were carried out using Eschbach's edge-enhancing algorithm, and the following problems were found:

1. The edge-enhancement effect depends on not only the brightness difference of adjacent pixels but also on the input pixel brightness itself. It causes an off-set dependent edge-enhancement effect.
2. The edge-enhancement effect is degraded for dark or bright pixels. (Experimental results for this phenomenon are discussed at the end of this section.) As the pixel value approaches 0 or 255, the edge-enhancement effect rapidly decreases.
3. As K increases (especially when $K \geq 5$), thick-edged artifacts become more visible, making the edge-enhanced image unnatural.
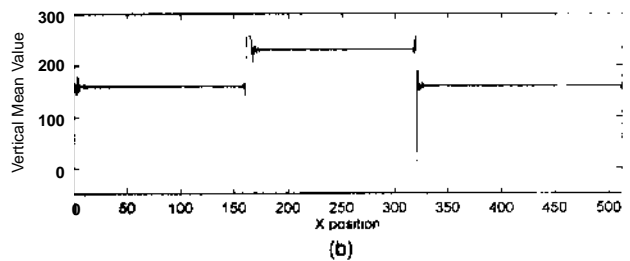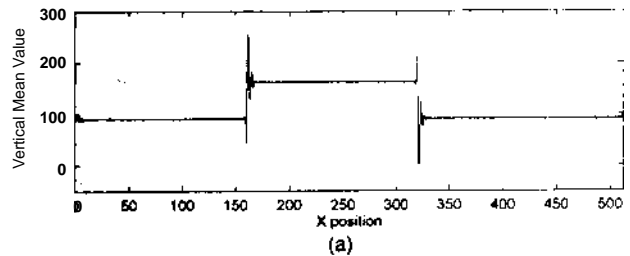

Figure 1. The l-D plot of edge-enhancement effects for different off-sets. Gray level changes (a) 93-163-93 and (b) 160-230-160.

These problems are shown by several experimental results in Sec. 5. We have experimented with the method for measuring the edge-enhancement effect, as illustrated in Fig. 1. This experiment was performed in the same manner as was done in Ref. 9. Two test images [Figs. 1(a) and 1(b)] have 1000 vertical lines over a band, which consists of three equally divided areas with levels of 93-163-93 and 160-230-160. Therefore the center of the images will be brighter than the sides, which will be darker according to the numbers above. Note that their brightness difference is 70.

After performing Eschbach's EDF, the vertical average of the output image is plotted in Fig. 1. In this experiment, though the gray-level differences of the edges in each image are the same (70), their edge characteristics are different. The edge enhancement also depends on the input pixel brightness itself. This is undesirable for the edge-enhancement characteristics.

4 Analysis of the Distribution of Error Sum and the Proposed Algorithm

4.1 The Distribution of Error Sum

The error sum E_s, which is diffused from adjacent pixels to modify the current pixel brightness, is expressed as

$$E_s(x,y) = \frac{\sum_{i,j} \alpha_{i,j} \cdot E(x - i\Delta x, y - j\Delta y)}{\sum_{i,j} \alpha_{i,j}}. \quad (7)$$

This error sum and the original input pixel brightness are added and used for generating a binary output pixel. The range of error sum distribution in Eschbach's algorithm is derived from Eqs. (1) through (6) and is given as

$$T_0 - 255 - (K - 1) \cdot I(x,y) < E_s(I) < T_0 - (K - 1) \cdot I(x,y) . \quad (8)$$

The range of the error sum varies according to the input pixel brightness. From now on, $E_s(I)$ instead of $E(x,y)$ will be used to represent the dependency on the input-pixel brightness. To observe the real situation, 256 sample sequence images with different gray levels (0-255) are generated. The image sizes for the x and y directions are 64 and 512 pixels, respectively. Eschbach's edge-enhanced EDF is applied to these test images and the range of the error sum distribution is investigated. For this experiment, the first 10 lines as well as the 5 left-most and right-most pixels of each line are not considered. Note that the error sum $E_s(I)$ in this experiment is generated from constant images not from images having an edge region.

The error sum distribution (the possible error sum values) for 256 constant gray-level images is shown in Fig. 2. The horizontal axis of Fig. 2 is the input image brightness. Note that the occurrence of the error sum for the input pixel brightness is shown in Fig. 2. Except near the 0 or 255 input brightness, the error sum exists in the region defined in Eq. (8). When the error sum exists in the range given by Eq. (8), the quality of the binary out-

put image is good in Eschbach's algorithm. When the image input is near black (0) or white (255), the error sum does not exist in the linear region specified by Eq. (8), and good binary output image quality cannot be obtained. For explaining the nonlinear region of the error sum distribution near 0 or 256, the principle of the edge enhancement needs to be explained.
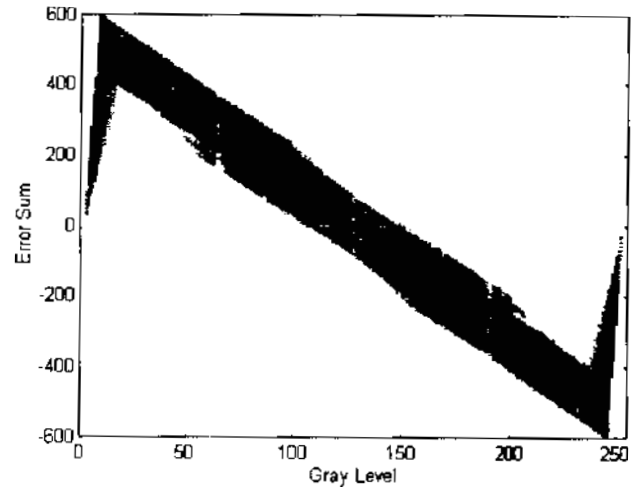

Figure 2. The error sum distribution depending on the gray levels of 256 constant images.

Consider an example image that has two areas of brightness I_1 and I_2 as shown in Fig. 3. For processing a constant brightness area (I_1), or slowly varying area, possible error sum values are around E_1. But when the EDF processing reaches a pixel with a quite different brightness (I_2), the error sum (E_1) stabilized in the I_1 area is quite different from the error sum (E_2), where the input brightness I_2 can be reproduced properly. Note that the proper range of the error sum is $E_2 \pm \Delta E$ for reproducing a constant I_2 image. Therefore, the error sum (E_1) has to move toward a new error sum (E_2) as Eschbach's EDF process continues. The transition speed of the error sum depends on the K value: When K is large, the speed is slow.

When the error sum reaches a new value E_2, continuous-tone image I_2 can be represented well. We need to look at the error-adapting amount that is diffusing into the adjacent pixels for the given input $I(x,y)$. It is written

$$E(x,y) = I_c(x,y) - O_b(x,y)$$
$$= E_s(I) + [I(x,y) - O_b(x,y)]. \quad (9)$$

As shown in this equation, the error-adapting amount is equal to the difference between the input and the output brightness. It is 0 for the input brightness 0 or 255, and it is small for the input pixel values near 0 or 255. This means the adaptation to a new error sum is slow for those input brightnesses. Therefore, many of the same binary output pixels are produced until they reach a new stable error sum value. Now the reason for the problems mentioned in Sec. 3 is understood.
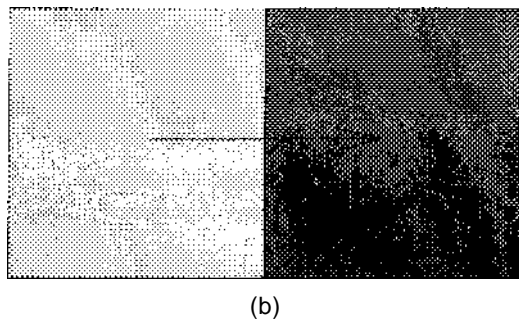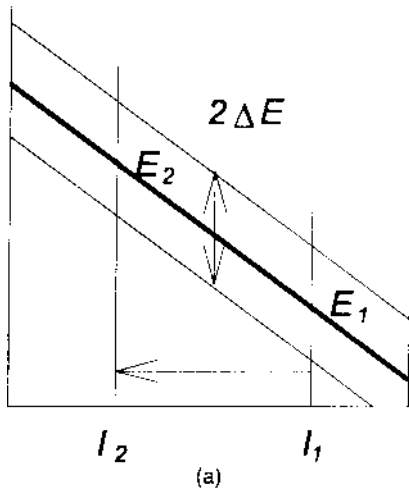
(a)

(b)

Figure 3. An illustration of error sum references for two different input brightness. Brightness change of I_1 to I_2 causes the error sum to move from around E_1 to around E_2.
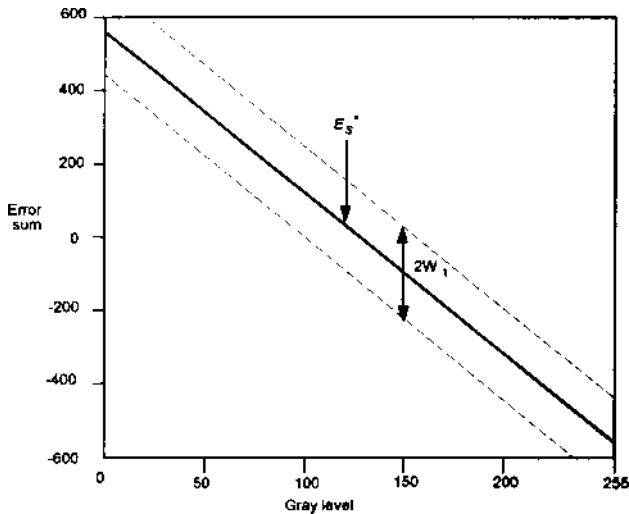

Figure 4. The relationship of the error sum displacement, reference error sum, and edge and nonedge regions.

By using these phenomena, it is easy to distinguish whether a pixel is in the normal or edge region. The error sum can be used for distinguishing whether a pixel lies in the edge region or not. The center value of the error sum distribution in Eq. (8) is called the *reference*

error sum E_s^*. It is linear to the input pixel brightness and derived from Eq. (8) as

$$E_s^*(I) = (K-1) \cdot (255/2 - I). \qquad (10)$$

The reference error sum is a mean value of the error sum for an input brightness $I(x,y)$. The difference between the calculated error sum and the reference error sum in Eschbach's EDF process is defined as the *error sum displacement* (*W*). These two defined values are explained in Fig. 4.

During the edge-enhanced EDF process, the reference error sum is automatically determined by Eq. (8). For the normal-region pixels, the displacement is expected to be small. For the edge region, the displacement tends to be large. We propose to define a threshold, named an *error sum displacement threshold* W_t, for detecting a pixel whether the pixel is on the edge region or not. When the error sum displacement W is not larger than W_t, the pixel is in the normal region; otherwise, it is in the edge region. By using this threshold, it is experimentally proved that the edge and normal regions are distinguished well.[13] Here, we propose a new edge-enhanced EDF for improving the edge characteristics of Eschbach's algorithm.

4.2 A New Edge-Enhanced Error Diffusion Algorithm

A block diagram of the proposed algorithm is shown in Fig. 5 and can be explained as follows:

1. If the pixel does not belong to the edge region, apply Eq. (9) for the error calculation.
2. Otherwise, a new error calculation is applied as shown in Eq. (11). A large error-adapting amount is used for a fast transition to a new reference error sum.

$$E_{NEW} = \begin{cases} E_s(I) + C & \text{when} \quad O_b = 255 \text{(white)} \\ E_s(I) - C & \text{when} \quad O_b = 0 \text{(black)} \end{cases}. \qquad (11)$$
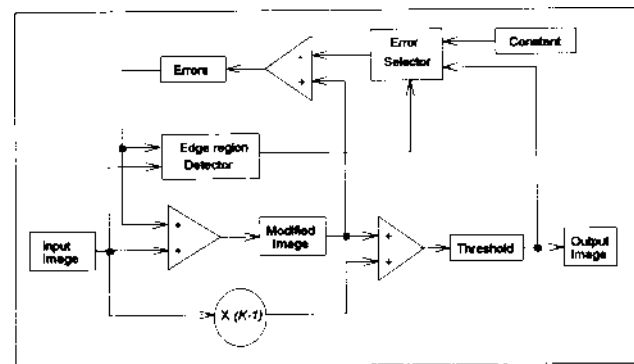

Figure 5. Block diagram of the new proposed algorithm. Edge region detector and error selection are added to Eschbach's algorithm.

In this equation, a constant C is added or subtracted to the diffused error. The binary output for this edge-

region pixel is determined as in Eschbach's algorithm. When the brightness differences are the same, no matter how much the offsets are, the amount of adaptation is the same. Therefore, the same amount of edge enhancement can be obtained.
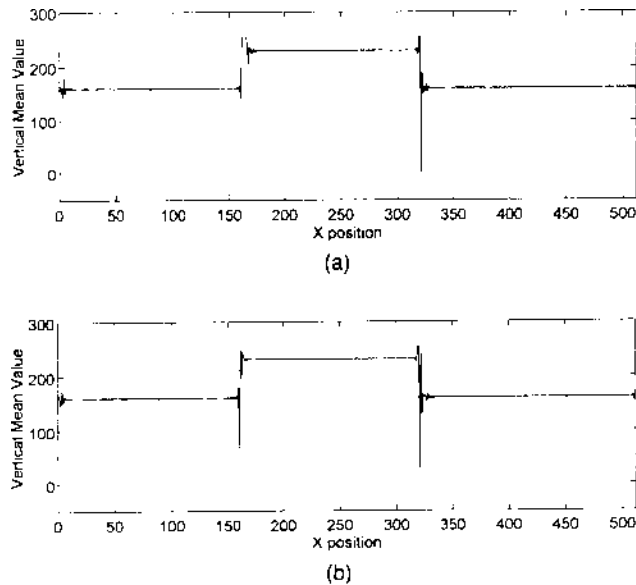

Figure 6. Comparison of the edge-enhancement effect for 160-230-160 brightness change. Results of (a) Eschbach's algorithm and (b) the proposed algorithm.

5 Discussion of the Experimental Results

The experiments of Eschbach's and the proposed edge-enhancement algorithms were carried out by using $K = 5$ and $W_t = 140$. The edge-adapting amount C was 200. First, the edge-enhancement effect was investigated by using the experiment of Fig. 3 in Sec. 3. The result in Fig. 6 shows that the edge characteristics are less influenced by the offset in the proposed method than in Eschbach's method.

The error sum distribution for the proposed method was obtained by using the 256 constant images with different gray levels. The result obtained is shown in Fig. 7. The proposed algorithm has a much wider linear region in the error sum distribution plot.

Two 400×400 and 600×400 experimental images were chosen for measuring the improvements. To see the offset-independent edge-enhancement effect, a test image is generated, as shown in Fig. 8(a). There are six patterns made of links, characters, and square blocks with brightnesses of 0, 51, 102, 128, 153, and 204. Eschbach's algorithm and the new algorithm are applied to the images for comparison. The following differences are shown in Figs. 8(b) and 8(c):

1. Characters in different gray backgrounds are enhanced in Fig. 8(c) compared to those in 8(b). When the brightness of a character and its background is biased near to 0 or 256, the enhancement is apparent.

2. A thick-edged artifact of the upper rectangle [the gray 51 of Fig. 8(b)] is reduced in Fig. 8(c).
3. The edges of the upper left corner of the upper rectangle (the gray 128 and 153) are enhanced in Fig. 8(c). But in Fig. 8(b), they are not enhanced because the brightness of the background of the rectangle is 255.
4. In Fig. 8(b), the upper left parts of the rectangle boxes or lines with brightnesses of 153 or 204 are distorted.
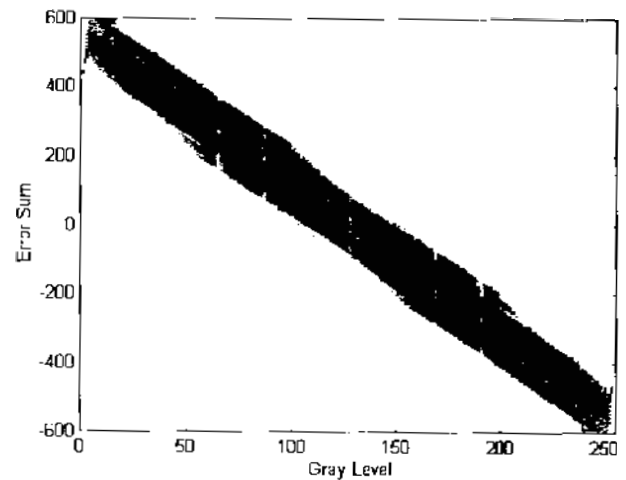

Figure 7. The relationship between the input pixel brightness and the distribution of error sum in the proposed algorithm.

The reason for the effect in item 4 can be explained as follows. The background is white (255). The error adaptation for the white (255) background is 0 [see Eq. (9)]. The amount of error sum made during the output of the pattern's lower part with brightnesses of 51 and 102 is not reduced on the white (255) background. It decreases after reaching the 153 and 204 input signal. Therefore, the error sum characteristics of this area are the same as when the edge of 51 reaches 153 or 102 reaches 204 directly. In the proposed method there are no such artifacts.

The proposed algorithm is also applied to the mobile image. The thick-edged artifact is reduced as shown in Fig. 9(c). Overall image quality is much improved in the proposed method. The thickness of the artifact can be adjusted by controlling C.

6 Conclusions

Edge-enhanced binarization is important because it allows images to be printed with a binary output device and also compensates for the low pass filtering effect of a scanner. It can be a cost-effective solution. Among several edge-enhanced EDF algorithms, Eschbach's is the most practical algorithm. It can be implemented with minimal changes from the normal EDF.

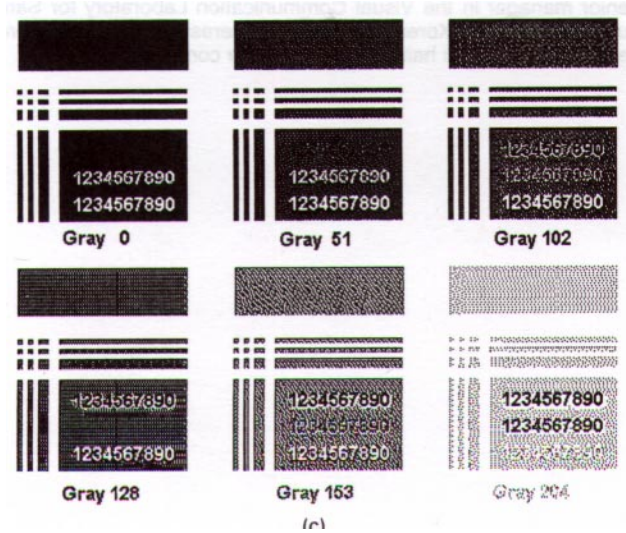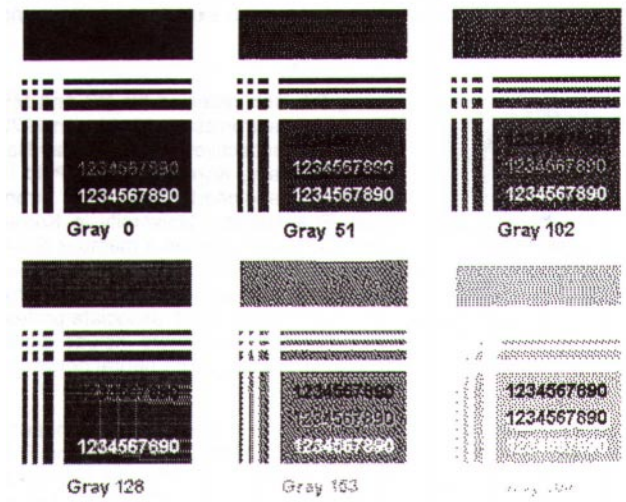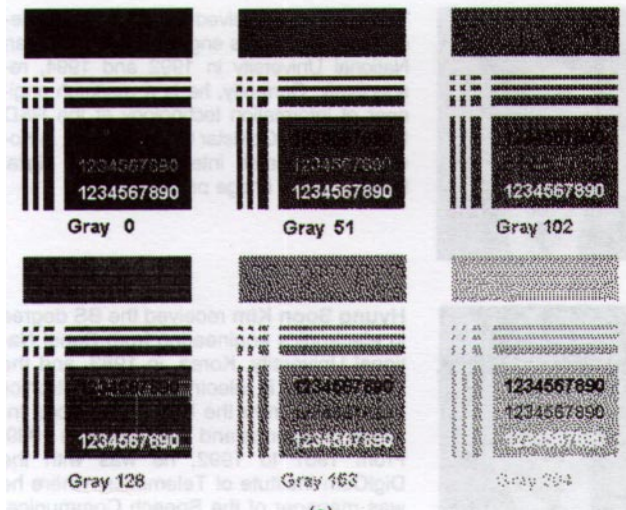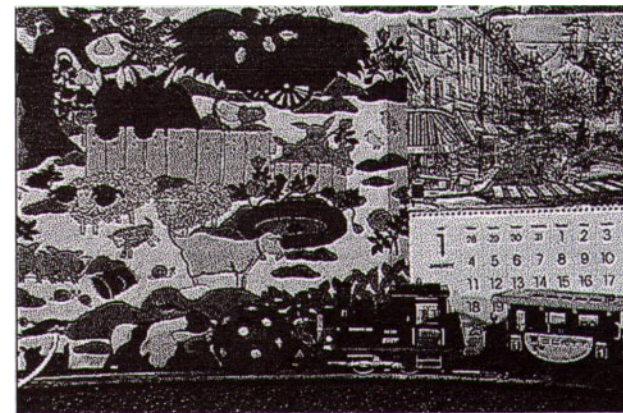In this paper, Eschbach's edge-enhancement mechanism was analyzed. It was found that the thick-edged

Figure 9. The results of edge-enhanced error diffusion of the mobile image by using (a) the original EDF (K = 1), (b) Eschbach's algorithm (K = 5), and (c) the proposed algorithm (K = 5).

Figure 8. The results of edge-enhanced error diffusion of the test image: (a) original EDF(K = 1), (b) Eschbach's algorithm (K = 5), and (c) the proposed algorithm (K= 5).

artifact depends on the input pixel brightness, which is caused by the different amount of error adaptation for each brightness. A transition to a new reference error sum from an old one is slow, thus a thick-edged artifact is produced.

The brightness of the current pixel, the reference error sum for the brightness, and the error sum displacement threshold are defined and used for classifying the regions of the pixel. After classifying the region of the pixel, different equations are applied for calculating the error of the pixel. In the proposed algorithm, the edges with white (255) or backgrounds are enhanced well and the thick-edged artifact is reduced. Depending on the specific applications, the error sum displacement threshold can be adjusted. The error adapation constant C for the edge-region pixel can also be adjusted.

For implementation, the proposed algorithm requires only a small amount of additional calculations (two comparison operations) and modifications to the original EDF architecture. This can be easily used for the design of a digital copier or facsimile machine.

References

1. R. W. Floyd and L. Steinberg, "An adaptive algorithm for spatial grey scale," *Proc. Soc. Inf. Disp.* **17**, 75–77 (1976).
2. B. B. Bayer, "An optimum method for two-level rendition of continuous-tone pictures," *Proc. IEEE Int. Conf Commun. Conference Record* **26**, 11–15 (1973).
3. R. Ulichney, *Digital Halltoning*, Chap. 8, MIT Press, Cambridge, MA (1987).
4. R. Eschbach and K. T. Knox, "Error diffusion algorithm with edge enhancement." *J. Opt. Soc. Am. A* **8**(12), 1844–1850 (1991).
5. M. Analoui and J. P. Allebach, "Model based halftoning using direct blnary search." *Proc. SPIE* **1666**, 96–108 (1992).
6. J. Sullivan, R. Miller, and G. Pios, "Image halftoning using a visual model in error diffusion," *J. Opt. Soc. Am. A* **10**(8), 1714–1724 (1993).
7. T. Mitsa and K. J. Parker, "Digital halftoning technique using a blue noise mask," *J. Opt. Soc. Am. A* **9**, 1920–1929 (1992).
8. K.T. Knox, "Error image in error diffusion," *SPIE Proc.* **1657**, 268–279 (1992).
9. K. T. Knox and R. Eschbach, "Threshold modulation in error diffusion," *J. Electron. Imaging* **2**(3), 185–192 (1993).
10. M, Broja, F. Wyrowski, and O. Bryngdahl, "Digital halftoning by carrier and spectrum control," *Opt. Commun.* **69**, 205–210 (1989).
11. J. H. Kim, G. S. Kang, S. K. Kim, J. W. Lee, B. W. Lee, Y. S. Kim, S. P. Cho, and S. H. Ha, "Development of 1-chip application-specific DSP for the next generation FAX image processing," *J. Korean Inst. Telematics Electron.* **31-B**, 30–39 (1994).
12. C. Billotet-Hoffmann and O. Bryngdahl, "On the error diffusion technique for electronic halftoning," *Proc. Soc. Inf. Disp.* **24**, 253–258 (1983).
13. T. I. Chung, H. S. Kim, K. S. Son, and J. H. Kim, "Edge detection with error sum in error diffusion," *The Korean Institute of Telematics and Electronics, Society in Pusan and Kyungnamn*, Autumn, p. 62 (1993).

✳ Previously published in the *Journal of Electronic Imaging,* **4**(2) pp. 172–178, 1995.